GFZ
Helmholtz-Zentrum
POTSDAM

Originally published as:

Steinhöfel, G., Horn, I., von Blanckenburg, F. (2009): Matrix-independent Fe isotope ratio determination in silicates using UV femtosecond laser ablation. - Chemical Geology, 268, 1-2, 67-73

DOI: 10.1016/j.chemgeo.2009.07.010

Matrix-independent Fe isotope ratio determination in silicates using UV femtosecond laser ablation

Chemical Geology (2009), *doi:10.1016/j.chemgeo.2009.07.010*

Grit Steinhoefel[a]*, Ingo Horn[a], and Friedhelm von Blanckenburg[b]

[a]Institut für Mineralogie, Universität Hannover, Callinstr. 3, D-30167 Hannover, Germany
[b]Deutsches GeoForschungsZentrum GFZ, Telegrafenberg, D-14473 Potsdam, Germany

*Corresponding author. E-mail address: g.steinhoefel@mineralogie.uni-hannover.de

Abstract

UV femtosecond laser ablation coupled to MC-ICP-MS provides a promising *in situ* tool to investigate elemental and isotope ratios by non-matrix-matched calibration. In this study, we investigate Fe isotope composition in siliceous matrices including biotite, hornblende, garnet, fayalite and forsterite (San Carlos Olivine), and an oceanic Fe-Mn crust using the iron reference material IRMM-014 for calibration. To test the accuracy of the laser ablation data, Fe isotope compositions were obtained independently by solution ICP-MS after chromatographic separation of Fe. Sample materials with low Cr content, i.e. biotite, hornblende, fayalite and the Fe-Mn crust, reveal $\delta^{56/54}$Fe and $\delta^{57/54}$Fe values that agree with those from solution ICP-MS data within the measured precision. For high Cr concentration (^{54}Cr/^{54}Fe > 0.0001), i.e. in the garnet and forsterite sample, $\delta^{56/54}$Fe and $\delta^{57/54}$Fe values were derived from ^{57}Fe/^{56}Fe ratios as correction of the isobaric interference of ^{54}Cr on ^{54}Fe is unsatisfactory. This approach provides accurate results for both minerals. Moreover, the garnet crystal exhibits isotopic zonation with differences of 0.3‰ in $\delta^{56/54}$Fe showing that substantial heterogeneities exist in high-temperature metamorphic minerals. Multiple analyses of homogeneous sample materials reveal a repeatability of 0.1‰ (2 SD) for $\delta^{56/54}$Fe and 0.2‰ (2 SD) for $\delta^{57/54}$Fe, respectively. This study adds to the observations of Horn et al. (2006) who have shown that the determination of Fe isotope ratios in various matrices including iron alloys, iron oxides and hydroxides, iron sulfide and iron carbonates can be performed with high accuracy and precision at high spatial resolution using UV femtosecond laser ablation ICP-MS. These results demonstrate that femtosecond laser ablation ICP-MS is a largely matrix-independent method, which provides a substantial advantage over commonly employed nanosecond laser ablation systems.

1. Introduction

In the past two decades, laser ablation (LA) in conjunction with inductively coupled plasma mass spectrometry (ICP-MS) has become a powerful *in situ* micro-analytical technique with broad applications in elemental and isotope ratio analysis. Today, most laser ablation systems operate in the UV range with a pulse duration of several nanoseconds (1 ns = 10^{-9} s). However, a major drawback of this technique is laser-related elemental and isotope fractionation, which introduces a strong matrix-dependency into the results (e.g. Sylvester, 2008). To control this effect, matrix-matched calibration standards are required. For geological applications, this approach is not always practical, because sample materials cover a large spectrum of matrices. Recent developments in LA employ lasers with shorter pulse durations ranging from ~60 to several hundreds of femtoseconds (1 fs = 10^{-15} s) (see reviews of Fernández et al. (2007) and Horn (2008)). The use of fs pulses for ablation provides significant improvements with respect to laser-induced and particle-size related fractionation so that non-matrix-matched calibration turns out to be feasible. Femtosecond LA-ICP-MS using non-matrix-matched calibration has been successfully applied to the analysis of element ratios, i.e. Zn/Cu, Pb/U and U/Th (Bian et al., 2005; 2006; González et al., 2004; Horn and von Blanckenburg, 2007; Koch et al., 2006; Mozna et al., 2006; Poitrasson et al., 2003) and of isotope ratios of heavy stable isotope systems, i.e. Cu, Fe and Si (Chmeleff et al., 2008; Horn and von Blanckenburg, 2007; Horn et al., 2006; Ikehata et al., 2008; Steinhoefel et al., 2009). The measurement of heavy stable isotope ratios is particularly challenging as the natural mass-dependent fractionation is very small, in the range of parts per thousand, which requires highly precise and accurate analysis. For instance, the natural variation in $\delta^{56/54}$Fe is about 5‰ (e.g. Dauphas and Rouxel, 2006). The absence of matrix-effects has been demonstrated for Fe isotope ratio determinations by UV fs LA coupled to a multiple collector ICP-MS (MC-ICP-MS) for a variety of matrices including native iron, iron alloys, iron sulfides, iron carbonates, iron oxides and hydroxides using the isotopically certified iron reference material IRMM-014 for calibration (Horn et

al., 2006). A similar approach demonstrates the matrix-independency for the determination of Si isotope ratios in siliceous materials including pure silicon, quartz, olivine and diopside by using the quartz reference standard NBS28 for calibration (Chmeleff et al., 2008). Non-matrix-matched calibration using near IR-fs-LA has also been successfully applied for the determination of Cu isotope ratios in Cu-rich minerals including cuprite, chalcocite and chalcopyrite by using the pure copper standard NIST-SRM 976 (Ikehata et al., 2008).
In this study, we show that accurate and precise Fe isotope ratios can be determined in silicate minerals using UV fs LA coupled to a MC-ICP-MS, which is a substantial advancement considering that 90% of the Earth's surface consists of silicates. Olivine (fayalite and forsterite), hornblende, biotite, garnet and complex matrices such as Fe-Mn crusts have been analysed using the iron reference material IRMM-014 for calibration. In these sample materials, the complexity of the matrix and the low Fe concentrations provide a formidable challenge.

2. Method

The in-house built fs LA system at the Leibniz University of Hannover is based on a 100 fs Ti:sapphire regenerative amplifier system (Spectra Physics Hurricane I, USA) with a fundamental wavelength of 785 nm, which is consecutively frequency-quadrupled providing an output laser beam in the deep UV region at 196 nm with a pulse energy of 0.02 mJ. Sample and standard materials can be placed as thin sections or as polished sections in a sample cell with an integrated fused silica window, which has three gas inlets and one outlet and a volume of 30 cm^3. The sample cell is mounted on a New Wave XP sample stage for visualization and precise positioning. The ablation rate for silicates is about 1.5 nm per pulse (Chmeleff et al., 2008). More details on the laser ablation system are given by Horn and von Blanckenburg (2007). The UV fs LA system is coupled to a ThermoFinnigan Neptune MC-ICP-MS, which is equipped with conventional Ni skimmer and sampler cones running under standard conditions (Table 1). The aerosol is transported to the mass spectrometer using He as carrier gas and is mixed with Ar gas before entering the torch. Fe isotope ratios were determined following the analytical protocol of Horn et al. (2006). The ThermoFinnigan Neptune MC-ICP-MS provides high mass resolution, which is able to resolve all molecular interference on the Fe isotopes excluding isobaric isotope interferences. The instrumental mass resolution was ~8000 defined as $m/\Delta m$, where m is the mass of the ion of interest and Δm is the mass difference between its 5 and 95% peak height. As well as the Fe isotopes ^{54}Fe, ^{56}Fe, ^{57}Fe and ^{58}Fe, ^{52}Cr and ^{60}Ni were measured by Faraday cups in static collection mode to correct for isobaric interferences of ^{54}Cr on ^{54}Fe and ^{58}Ni on ^{58}Fe. The correction modes for the LA data are identical to the method described and tested in detail for solution ICP-MS data by Schoenberg and von Blanckenburg (2005).
The analyses were performed using the standard-sample-bracketing technique and the iron reference material IRMM-014. This external calibration technique involves the analysis of a reference standard of known isotope composition prior to and after the measurement of the sample material to correct for the instrumental mass discrimination and its temporal drift. The instrumental drift has to be less than 0.1‰ on the $^{56}Fe/^{54}Fe$ ratio between standard measurements to minimize the interpolation error. To stabilize measurement conditions for the analysis of silicates, the siliceous sample material was continuously ablated for about 1 h prior to analysis. This procedure conditions the interface region, which stabilizes the interaction of the ions with skimmer and sampler cones through a coating. Conditioning enables alternating analyses of silicate and Fe metal matrices, which is required for calibration by the sample-standard-bracketing method and therefore precise Fe isotope measurements. Without preconditioning, the instrumental conditions are highly unstable with a drift of several permils of the $^{56}Fe/^{54}Fe$ ratio between standard measurements.
To explore the behaviour of different siliceous matrices, we analysed the following sample materials: olivine (fayalite and forsterite), biotite, hornblende, garnet and a Fe-Mn crust. Olivine with fayalite composition is from the contact metamorphosed Biwabik Iron Formation (USA) (sample E in Frost et al. (2007)). San Carlos Olivine (SC Olivine), a well-established $\delta^{18}O$ mineral standard, is of forsterite composition and is often used in experimental petrology (e.g. Costa and Chakraborty, 2008; Galer and O'Nions, 1989; Holzheid and Grove, 2002). The biotite sample B-4B is a mineral standard for K-Ar dating (Flisch, 1982). The hornblende sample Siss 3 is from the Bergell tonalite in the southeast Central Alps (Villa and von Blanckenburg, 1991). The garnet sample is a piece from the rim of a single idiomorphic almandine crystal of about 5 cm in diameter formed in schist. The metamorphic grade of this sample is amphibolites facies as indicated by chlorite, mica and garnet in schist. The garnet crystal exhibits a homogeneous chemical composition (Table 2). Mineral inclusions are rare and were avoided for Fe isotope analysis. The Fe-Mn crust (cruise VA13/2, sample 327 KD) is from the Central Pacific (von Stackelberg et al., 1984) and was analysed at its surface. The in-house metal standard Puratronic (Johnson Matthey) is frequently analysed as control sample during our laser ablation sessions. The major element composition of the sample materials is reported in Table 2.
Sample materials and iron reference material IRMM-014 were analysed in raster-mode using a spot diameter of ~30 μm. The acquisition parameters were set to acquire 50 to 80 cycles per analysis, with a cycle integration time of 2 s. The total consumption is about 45 ng Fe for an analysis on pure iron (reference material IRMM-014) and an average signal of 10 V for ^{56}Fe on a faraday cup equipped with a $10^{11}\Omega$ resistor (Steinhoefel et al., 2009).

Analysis of minerals with lower Fe concentrations requires corresponding higher material consumptions. On-peak-zero measurements were usually not subtracted as the background signal on mass ^{56}Fe was less than 1.5 mV compared to signal intensities of 8 to 12 V on a 10^{11} Ω resistor when analysing the sample material. Exceptions are biotite and forsterite, where signal intensities on mass ^{56}Fe of only 5 V were achieved. In these cases, the background levels for all detected isotopes were measured for 30 cycles prior to each analysis by closing the laser shutter and then subtracted from each measured cycle. To compensate for different Fe concentrations and light absorption efficiencies between sample and standard materials, Fe signal intensities were matched by applying different laser repetition rates in order to reveal similar signal to background ratios making background correction unnecessary (Table 3). Multiple analyses were performed for each sample to investigate the external repeatability. Each sample was analysed in one to three measuring sessions within 12 months.

To prove the accuracy of the LA data, Fe isotope composition of the sample materials were obtained independently by solution nebulization ICP-MS following the procedure described in Schoenberg and von Blanckenburg (2005). Forsterite, biotite, garnet and hornblende were digested in HF-HNO_3. The Mn-Fe crust was dissolved in 6 mol/L HCl. Fe was separated by anion-exchange chromatography. For the Fe-Mn crust, Fe was additionally precipitated with $NH_4(OH)$ after anion-exchange chromatography to remove residual transition metals. The Fe isotope compositions were then determined on a ThermoFinnigan Neptune MC-ICP-MS from solutions by the standard-sample-bracketing method using the iron reference material IRMM-014. The external reproducibilities at the 95% confidence level of solution nebulization ICP-MS for $\delta^{56/54}Fe$ and $\delta^{57/54}Fe$ are 0.049‰ and 0.071‰, respectively (Schoenberg and von Blanckenburg, 2005).

LA and solution data are reported as $\delta^{56/54}Fe$, $\delta^{57/54}Fe$ and $\delta^{57/56}Fe$ values relative to IRMM-014, e.g. for $\delta^{56/54}Fe$:

$$\frac{\delta^{56/54}Fe}{‰} = \left(\frac{{}^{56}Fe/{}^{54}Fe_{Sample}}{{}^{56}Fe/{}^{54}Fe_{IRMM-014}} - 1 \right) * 1000$$

3. Results

All LA data of the individual samples are presented in three-isotope plots as $\delta^{56/54}Fe$ versus $\delta^{57/54}Fe$ together with the independently obtained solution ICP-MS data as reference values (Fig. 1). Mean Fe isotope data of fs LA-ICP-MS and solution ICP-MS are summarized in Table 4. Accurate data have to plot along the mass-dependent fractionation line defined by the mass differences with a slope of 1.4881 and should agree with the solution ICP-MS values within their respective precision. Data that plots elsewhere in the diagram are affected by isobaric interferences.

The fayalite sample exhibits a mean LA $\delta^{56/54}Fe$ value of –0.19 ± 0.15‰ (2 SD, n = 8) compared to –0.18‰ in $\delta^{56/54}Fe$ obtained by solution ICP-MS (Fig. 1a). For the SC Olivine (fosterite) (Fig. 1b), the LA data yielded lower $\delta^{56/54}Fe$ values than solution ICP-MS giving mean $\delta^{56/54}Fe$ values of -0.32 ± 0.13‰ (2 SD, n = 18) and –0.04‰, respectively. Moreover, not all LA data plot on the fractionation line giving evidence for isobaric interferences. Garnet revealed a mean LA $\delta^{56/54}Fe$ value of –0.23 ± 0.34‰ (2 SD, n = 44) (Fig. 1c). Isotopic difference exists within the garnet crystal when comparing the data of the outer rim ('rim') giving a mean $\delta^{56/54}Fe$ value of –0.28 ± 0.13‰ (2 SD, n = 23) with data obtained in 2 cm distance from it ('interior'), which reveal a mean $\delta^{56/54}Fe$ value of –0.01 ± 0.30‰ (2 SD, n = 11), although its chemical composition is homogeneous. Some of the data points for garnet do not plot on the fractionation line. Solution ICP-MS obtained a $\delta^{56/54}Fe$ value of –0.18‰ for garnet. Biotite revealed a mean LA $\delta^{56/54}Fe$ value of 0.22 ± 0.15‰ (2 SD, n = 11) and a solution ICP-MS $\delta^{56/54}Fe$ value of 0.09‰ (Fig. 1d). For hornblende (Fig. 1e), the mean LA $\delta^{56/54}Fe$ value is -0.01 ± 0.11‰ (2 SD, n = 12), and solution ICP-MS revealed a $\delta^{56/54}Fe$ value of 0.08‰. LA-ICP-MS analyses of the surface of the Fe-Mn crust give a mean $\delta^{56/54}Fe$ value of –0.23 ± 0.10‰ (2 SD, n = 11) as compared to –0.30‰ in $\delta^{56/54}Fe$ obtained by solution ICP-MS (Fig. 1f). All data obtained for fayalite, biotite, hornblende and the Fe-Mn crust plot on the mass-dependent fractionation line.

4. Discussion

Matrix effects during LA-ICP-MS cause deviation from the assumed true Fe isotope composition, i.e. solution ICP-MS values. Well-known matrix-dependent processes for ns LA are 1) fractionation at the ablation site, which leads to non-stoichiometric aerosols (e.g. Eggins et al., 1998; Hergenröder, 2006; Košler et al., 2005) and 2) particle-size-related fractionation due to incomplete transport and ionisation of large particles in the ICP (e.g. Koch et al., 2002; Guillong et al., 2003). These effects, however, appear to be largely absent for fs LA (Garcia et al., 2008a, b; Horn and von Blanckenburg, 2007; Koch et al., 2004; 2005; Liu et al., 2004; Margetic et al., 2000; Saetveit et al., 2008; Wälle et al., 2008). Other matrix effects can be relevant for both ns and fs LA. For instance,

variable plasma-loads can affect the instrumental mass discrimination (e.g. Kroslakova and Guenther, 2007), which might arise from the requirement to match the intensities of Fe ion beams by adjusting the laser repetition rates between sample and standard material, thereby introducing a higher load of non-Fe ions for the sample.
Other effects are isobaric inferences, which can compromise the results. At high Cr concentration of the sample material, the isobaric interference of ^{54}Cr on ^{54}Fe limits the accurate determination of $^{56}Fe/^{54}Fe$ and $^{57}Fe/^{54}Fe$ ratios for the MC-ICP-MS measurements.

4.1. Isobaric Cr interference

The isobaric interference of ^{54}Cr on ^{54}Fe is corrected using the method described in Schoenberg and von Blanckenburg (2005) which, however, can become unsatisfactory at high Cr concentration. ^{52}Cr is measured to calculate ^{54}Cr by making the following assumptions, all of which introduce minor uncertainties: 1) the instrumental mass discrimination of Cr isotopes is calculated from $^{57}Fe/^{56}Fe$ ratio of samples relative to the certified IRMM-014 value, even though the instrumental mass discrimination might differ between these ratios (Albarède and Beard, 2004), 2) the $^{57}Fe/^{56}Fe$ ratio of the sample differs up to 1.5‰ from IRMM-014 and 3) the ratio $^{54}Cr/^{52}Cr$ is considered to be constant, although natural mass-dependent fractionation exists (e.g. Schoenberg et al., 2008). An incorrect Cr correction should result in data that does not follow the mass-dependent fractionation line in a $\delta^{56/54}Fe$ versus $\delta^{57/54}Fe$ plot, but a minor insufficient ^{54}Cr correction can easily escape notice. In a three-isotope plot, under- or over-correction shifts the data along a vector with the slope of 1, whereas the fractionation line has a slope of 1.4881. LA data can be shifted by about ± 0.2‰ in $\delta^{56/54}Fe$ and still appear within errors to plot along the fractionation line. This correction method has been demonstrated to be sufficient for solution ICP-MS data with low Cr concentrations and $^{54}Cr/^{54}Fe$ ratios up to 0.0001 (Schoenberg and von Blanckenburg, 2005). Therefore this correction was adopted with the same Cr limit for LA-ICP-MS in this study. The LA data of the samples fayalite, biotite, hornblende, and Fe-Mn crust reveal $^{54}Cr/^{54}Fe$ ratios of 0.0001 or lower, and agree with the solution ICP-MS data within their respective precision (Table 4). This demonstrates an adequate Cr correction for these samples and excludes other matrix-effects. The SC Olivine (forsterite) exhibits a $^{54}Cr/^{54}Fe$ ratio of 0.0011. The $\delta^{56/54}Fe$ data obtained by LA are on average 0.3‰ lower when compared to solution data giving evidence for under-correction of ^{54}Cr on ^{54}Fe (Fig. 1b, 2). Garnet revealed a similar $^{54}Cr/^{54}Fe$ ratio of 0.0010, but the data appear to be less affected on average. The mean LA $\delta^{56/54}Fe$ value does not differ significantly from the solution ICP-MS value (Fig. 1c). To circumvent this limitation for high Cr concentrations, $\delta^{56/54}Fe$ can be calculated from the unaffected $\delta^{57/56}Fe$ value by multiplying with a factor of 1.9944, which corresponds to the mass difference between ^{56}Fe and ^{54}Fe relative to the mass difference between ^{57}Fe and ^{56}Fe and an exponential fractionation law. For the SC Olivine, this approach reveals an inferred mean $\delta^{56/54}Fe$ value of –0.13 ± 0.30‰ (2 SD, n=18) as compared to –0.04‰ in $\delta^{56/54}Fe$ obtained by solution ICP-MS, which is consistent within its precision. The inferred mean $\delta^{56/54}Fe$ value for garnet is -0.17 ± 0.38‰ (2 SD, n=11), which agrees well with –0.18‰ in $\delta^{56/54}Fe$ revealed by solution ICP-MS.
For sample materials with a $^{54}Cr/^{54}Fe$ ratio higher than 0.0001, $\delta^{56/54}Fe$ values should be inferred from $\delta^{57/56}Fe$, since the Cr correction becomes unreliable. All analysed matrices yield accurate results within their precision after careful evaluation of the Cr correction. These results demonstrate that matrix effects are undetectable within the obtainable precision of 0.15‰ (2 SD).

4.2. Variable mass load in the ICP-MS

Variable ion loads in the mass spectrometer may be present if sample and standard material were ablated with different laser repetition rates in order to compensate for variable Fe concentrations of the materials (Table 3). Mass load induced-matrix effects in the mass spectrometer can result in variable instrumental mass discrimination and potentially occur for both ns and fs laser ablation (e.g. Horn and von Blanckenburg, 2007; Kroslakova and Guenther, 2007). A changing ion load might influence the space charge effect in the ICP, which describes the preferential extraction of heavy ions, and the extraction conditions in the ion optical system of the mass spectrometer. Despite the application of very different repetition rates and therefore highly variable mass loads (Table 3), this effect appears to be negligible as accuracy is maintained for all analysed samples.

4.3. Reproducibility and accuracy

The external repeatability of Fe isotope analysis for the various matrices has been determined by multiple analyses (n > 10), which have been obtained in one to three measuring sessions within a period of 12 months. For hornblende and the surface of the Fe-Mn crust, a precision of close to 0.10‰ was achieved in $\delta^{56/54}Fe$ (2 SD), which is identical to the precision obtained for pure iron (Puratronic) (Table 4) and other homogeneous materials, e.g. iron oxides and iron meteorites (Horn et al., 2006). Fayalite and biotite exhibit slightly increased standard deviations of ± 0.15‰ (2 SD), respectively. This results from low signal intensities for biotite, e.g. 5 V

on mass ^{56}Fe. The fayalite sample might be slightly heterogeneous in its Fe isotope composition. Although the fayalite crystallized at high temperatures during contact metamorphism in the Biwabik Iron Formation, it exhibits also slightly heterogeneous Fe concentrations (Frost et al., 2007). Because of high Cr concentrations relative to the Fe contents in SC Olivine and garnet, $\delta^{57/56}$Fe values are preferred. These values have a slightly increased uncertainty of 0.15‰ (2 SD) for SC Olivine due to the low Fe concentration. For $\delta^{56/54}$Fe values inferred from $\delta^{57/56}$Fe values, propagation doubles uncertainties. The increased errors for δ-values determined for garnet can be explained by a heterogeneous Fe isotope composition of the crystal, although its chemical composition is homogeneous. The outer rim of the crystal revealed a mean inferred $\delta^{56/54}$Fe values of –0.25‰, which differs significantly from 0.07‰ obtained in 2 cm distance from the rim (two-sample Student's *t*-test, 99% confidence level) (Table 3). This Fe isotope zonation in garnet indicates different growth stages of the crystal and shows that substantial Fe isotope heterogeneities exist in high-temperature metamorphic minerals.
The accuracy of the LA data is scrutinized by comparison with solution ICP-MS data for which samples have been subjected to chemical purification prior to analysis. All LA data yield within their respective precision (2 SD) identical results when compared with solution ICP-MS data demonstrating a high degree of matrix-independency for fs LA-ICP-MS (Fig. 3).

5. Conclusions

These results support the observations of Horn et al. (2006) and demonstrate that UV fs LA coupled to MC-ICP-MS provide highly precise and accurate Fe isotope data at high spatial resolution using non-matrix-matched calibration. This applies even for sample materials with complex matrices and low Fe concentrations (< 10wt.% FeO).

1) For the analysis of siliceous matrices, continuous ablation of the sample material prior to analysis establishes stable conditions by conditioning the interface region of the ICP-MS.
2) Due to the isobaric interference of ^{54}Cr on ^{54}Fe in the ICP-MS, a careful consideration of the Cr correction is necessary for sample materials with high Cr concentrations. $\delta^{57/56}$Fe values are preferred for sample materials with a ^{54}Cr/^{54}Fe ratio higher than 0.0001. Commonly used $\delta^{56/54}$Fe and $\delta^{57/54}$Fe values can be inferred by multiplying $\delta^{57/56}$Fe with the relative mass difference of the desired isotope ratio because of the mass-dependent fractionation behaviour of Fe isotopes, both in nature and during analytical mass discrimination.
3) The accuracy and reproducibility of Fe isotope have been verified for the following matrices: pure iron, iron meteorites, iron oxides and hydroxides, iron sulfides, iron carbonates, biotite, olivine (forsterite and fayalite), hornblende, garnet and a Fe-Mn crust (this study, Horn et al., 2006). All of which have been measured using non-matrix-matched calibration, which demonstrates that matrix effects are absent within the obtainable precision of 0.1‰ (2 SD) in $\delta^{56/54}$Fe and 0.2‰ (2 SD) in $\delta^{57/54}$Fe.

Femtosecond LA-ICP-MS provides an excellent tool to study Fe isotope variations *in situ* at high spatial resolution independent of the matrix while maintaining precision and accuracy. This capability opens a wide spectrum of applications allowing the investigation of Fe isotope variations in coexisting mineral phases in order to constrain processes in low and high temperature environments. An example for this type of application is the study of Fe isotopes in Precambrian banded iron formations to reconstruct their genesis (Steinhoefel et al., 2009). Precise Fe isotope analysis of silicate mineral phases is of particular interest when investigating processes in metamorphic and igneous rocks, which exhibit small variation in Fe isotope composition (e.g. Beard and Johnson, 2004; Poitrasson and Freydier, 2005; Schoenberg, 2009; Schuessler et al., 2007; 2009). The potential to explore high temperature processes becomes obvious considering the Fe isotope zonation with differences of 0.3‰ in $\delta^{56/54}$Fe discovered in garnet. Many applications using tracer studies in the material sciences now also appear to be possible.

Acknowledgements

We appreciate the support of this research by the DFG and New Wave Research. G.S. is grateful for a scholarship from the Leibniz University of Hannover. I. Villa provided the biotite sample B-4B. O. Dietrich kindly prepared the thin sections. W. Dziony is thanked for microprobe analyses. We thank an anonymous reviewer and F. Poitrasson for their constructive comments on the manuscript.

References

Albarède F., Beard B. L., 2004. Analytical methods for non-traditional isotopes. In: Johnson, C. M., Beard, B. L., Albarède, F. (Eds.), Geochemistry of Non-Traditional Stable Isotopes. Reviews in Mineralogy and Geochemistry, Mineralogical Society of America, Washington, pp. 113–152.

Beard B. L., Johnson C. M., 2004. Fe isotope variations in the modern and ancient earth and other planetary bodies. In: Johnson, C. M., Beard, B. L., Albarède, F. (Eds.), Geochemistry of non-traditional stable isotopes. Reviews in Mineralogy and Geochemistry, Mineralogical Society America, Washington, pp. 319-357.

Bian Q. Z., Garcia C. C., Koch J., Niemax K., 2006. Non-matrix matched calibration of major and minor concentrations of Zn and Cu in brass, aluminium and silicate glass using NIR femtosecond laser ablation inductively coupled plasma mass spectrometry. J. Anal. Atom. Spectrom. 21, 187-191.

Bian Q. Z., Koch J., Lindner H., Berndt H., Hergenröder R., Niemax K., 2005. Non-matrix matched calibration using near-IR femtosecond laser ablation inductively coupled plasma optical emission spectrometry. J. Anal. Atom. Spectrom. 20, 736-740.

Chmeleff J., Horn I., Steinhoefel G., von Blanckenburg F., 2008. In situ determination of precise stable Si isotope ratios by UV-femtosecond laser ablation high-resolution multi-collector ICP-MS. Chem. Geol. 249, 155-166.

Costa F., Chakraborty S., 2008. The effect of water on Si and O diffusion rates in olivine and implications for transport properties and processes in the upper mantle. Phys. Earth Planet. In. 166, 11-29.

Dauphas N., Rouxel O., 2006. Mass spectrometry and natural variations of iron isotopes. Mass Spectrom. Rev. 25, 515-550.

Eggins S. M., Kinsley L. P., Shelley J. M. G., 1998. Deposition and element fractionation processes during atmospheric pressure laser sampling for analysis by ICP-MS. Appl. Surf. Sci. 129, 278-286.

Fernández B., Claverie F., Pécheyran C., Donard O. F. X., 2007. Direct analysis of solid samples by fs-LA-ICP-MS. Trends Anal. Chem. 26, 951-966.

Flisch M., 1982. Potassium argon analysis. In: Odin, G. S. (Ed.), Numerical dating in stratigraphy. John Wiley, Chichester, pp. 151-158.

Frost C. D., von Blanckenburg F., Schoenberg R., Frost B. R., Swapp S. M., 2007. Preservation of Fe isotope heterogeneities during diagenesis and metamorphism of banded iron formation. Contrib. Mineral. Petrol. 153, 211-235.

Galer S. J. G., O'Nions R. K., 1989. Chemical and Isotopic Studies of Ultramafic Inclusions from the San Carlos Volcanic Field, Arizona: A Bearing on their Petrogenesis. J. Petrol. 30, 1033-1064.

Garcia C. C., Lindner H., von Bohlen A., Vadla C., Niemax K., 2008a. Elemental fractionation and stoichiometric sampling in femtosecond laser ablation. J. Anal. Atom. Spectrom. 23, 470-478.

Garcia C. C., Wälle M., Lindner H., Koch J., Niemax K., Günther D, 2008b. Femtosecond laser ablation inductively coupled plasma mass spectrometry: Transport efficiencies of aerosols released under argon atmosphere and the importance of the focus position. Spectrochim. Acta B 63, 271–276.

González J., Liu C., Mao X., Russo R. E., 2004. UV-femtosecond laser ablation-ICP-MS for analysis of alloy samples. J. Anal. Atom. Spectrom. 19, 1165-1168.

Guillong M., Horn I., Guenther D., 2003. A comparison of 266 nm, 213 nm and 193 nm produced from a single solid state Nd : YAG laser for laser ablation ICP-MS. J. Anal. Atom. Spectrom. 18, 1224-1230.

Hergenröder R., 2006. A model of non-congruent laser ablation as a source of fractionation effects in LA-ICP-MS. J. Anal. Atom. Spectrom. 21, 505-516.

Holzheid A., Grove T. L., 2002. Sulfur saturation limits in silicate melts and their implications for core formation scenarios for terrestrial planets. Am. Mineral. 87, 227-237.

Horn I., 2008. Comparison of femtosecond and nanosecond laser interactions with geological matrices and their influence on accuracy and precision of LA–ICP-MS data. In: Sylvester, P. J. (Ed.), Laser Ablation–ICP–MS in the Earth Sciences. Mineralogical Association of Canada Short Course Series, pp. 53-65.

Horn I., von Blanckenburg F., 2007. Investigation on elemental and isotopic fractionation during 196 nm femtosecond laser ablation multiple collector inductively coupled plasma mass spectrometry. Spectrochim. Acta B 62, 410-422.

Horn I., von Blanckenburg F., Schoenberg R., Steinhoefel G., Markl G., 2006. In situ iron isotope ratio determination using UV-femtosecond laser ablation with application to hydrothermal ore formation processes. Geochim. Cosmochim. Acta 70, 3677-3688.

Ikehata K., Notsu K., Hirata T., 2008. In situ determination of Cu isotope ratios in copper-rich materials by NIR femtosecond LA-MC-ICP-MS. J. Anal. Atom. Spectrom. 23, 1003-1008.

Koch J., Feldmann I., Jakubowski N., Niemax K., 2002. Elemental composition of laser ablation aerosol particles deposited in the transport tube to an ICP. Spectrochim. Acta, Part B 57, 975-985.

Koch J., Lindner H., Von Bohlen A., Hergenröder R., Niemax K., 2005. Elemental fractionation of dielectric aerosols produced by near-infrared femtosecond laser ablation of silicate glasses. J. Anal. Atom. Spectrom. 20, 901-906.

Koch J., Wälle M., Pisonero J., Guenther D., 2006. Performance characteristics of ultra-violet femtosecond laser ablation inductively coupled plasma mass spectrometry at similar to 265 and similar to 200 nm. J. Anal. Atom. Spectrom. 21, 932-940.

Koch J., von Bohlen A., Hergenröder R., Niemax K., 2004. Particle size distributions and compositions of aerosols produced by near-IR femto- and nanosecond laser ablation of brass. J. Anal. Atom. Spectrom. 19, 267-272.

Košler J., Wiedenbeck M., Wirth R., Hovorka J., Sylvester P., Míková J., 2005. Chemical and phase composition of particles produced by laser ablation of silicate glass and zircon - Implications for elemental fractionation during ICP-MS analysis. J. Anal. Atom. Spectrom. 20, 402-409.

Kroslakova I., Guenther D., 2007. Elemental fractionation in laser ablation-inductively coupled plasma-mass spectrometry: Evidence for mass load induced matrix effects in the ICP during ablation of a silicate glass. J. Anal. Atom. Spectrom. 22, 51-62.

Liu C., Mao X. L., Mao S. S., Zeng X., Greif R., Russo R. E., 2004. Nanosecond and femtosecond laser ablation of Brass: particulate and ICPMS measurements. Anal. Chem. 76, 379-383.

Margetic V., Pakulev A., Stockhaus A., Bolshov M., Niemax K., Hergenröder R., 2000. A comparison of nanosecond and femtosecond laser-induced plasma spectroscopy of brass samples. Spectrochim. Acta B 55, 1771-1785.

Mozna V., Pisonero J., Hola M., Kanicky V., Guenther D., 2006. Quantitative analysis of Fe-based samples using ultraviolet nanosecond and femtosecond laser ablation-ICP-MS. J. Anal. Atom. Spectrom. 21, 1194-1201.

Poitrasson F., Freydier R., 2005. Heavy iron isotope composition of granites determined by high resolution MC-ICP-MS. Chem. Geol. 222, 132-147.

Poitrasson F., Mao X. L., Mao S. S., Freydier R., Russo R. E., 2003. Comparison of ultraviolet femtosecond and nanosecond laser ablation inductively coupled plasma mass spectrometry analysis in glass, monazite, and zircon. Anal. Chem. 75, 6184-6190.

Saetveit N. J., Bajic S. J., Baldwin D. P., Houk R. S., 2008. Influence of particle size on fractionation with nanosecond and femtosecond laser ablation in brass by online differential mobility analysis and inductively coupled plasma mass spectrometry. J. Anal. Atom. Spectrom. 23, 54-61.

Schoenberg R., von Blanckenburg F., 2005. An assessment of the accuracy of stable Fe isotope ratio measurements on samples with organic and inorganic matrices by high-resolution multicollector ICP-MS. Int. J. Mass Spectrom. 242, 257-272.

Schoenberg, R, Marks, M A W, Schuessler, J A , von Blanckenburg, F , Markl, G, 2009. Fe isotope systematics of coexisting amphibole and pyroxene in the alkaline igneous rock suite of the Ilímaussaq Complex, South Greenland. Chem. Geol. 258 , 65-77.

Schuessler J. A., Schoenberg R., Behrens H., von Blanckenburg F., 2007. The experimental calibration of the iron isotope fractionation factor between pyrrhotite and peralkaline rhyolitic melt. Geochim. Cosmochim. Acta 71, 417-433.

Schuessler J. A., Schoenberg R., Sigmarsson O., 2009. Iron and lithium isotope systematics of the Hekla volcano, Iceland - Evidence for Fe isotope fractionation during magma differentiation. Chem. Geol. 258, 78-91.

Steinhoefel G., Horn I., Blanckenburg F., 2009. Micro-scale tracing of Fe and Si isotope signatures in banded iron formation using femtosecond laser ablation. Geochim. Cosmochim. Acta 73, 5343-5360.

Sylvester P. J., 2008. Martix effects in laser ablation ICP-MS. In: Sylvester, P. J. (Ed.), Laser Ablation–ICP–MS in the Earth Sciences. Mineralogical Association of Canada Short Course Series, pp. 67-78.

Villa I. M., von Blanckenburg F., 1991. A hornblende ^{39}Ar-^{40}Ar age traverse of the Bregaglia tonalite (southwest Central Alps). Schweiz. Miner. Petrog. 71, 73-87.

von Stackelberg U., Kunzendorf H., Marchig V., Gwozdz R., 1984. Growth history of a large ferromanganese crust from the equatorial north Pacific nodule belt. Geologisches Jahrbuch A75, 213-235

Wälle M., Koch J., Guenther D., 2008. Analysis of brass and silicate glass by femtosecond laser ablation inductively coupled plasma mass spectrometry using liquid standard calibration. J. Anal. Atom. Spectrom. 23, 1285-1289.

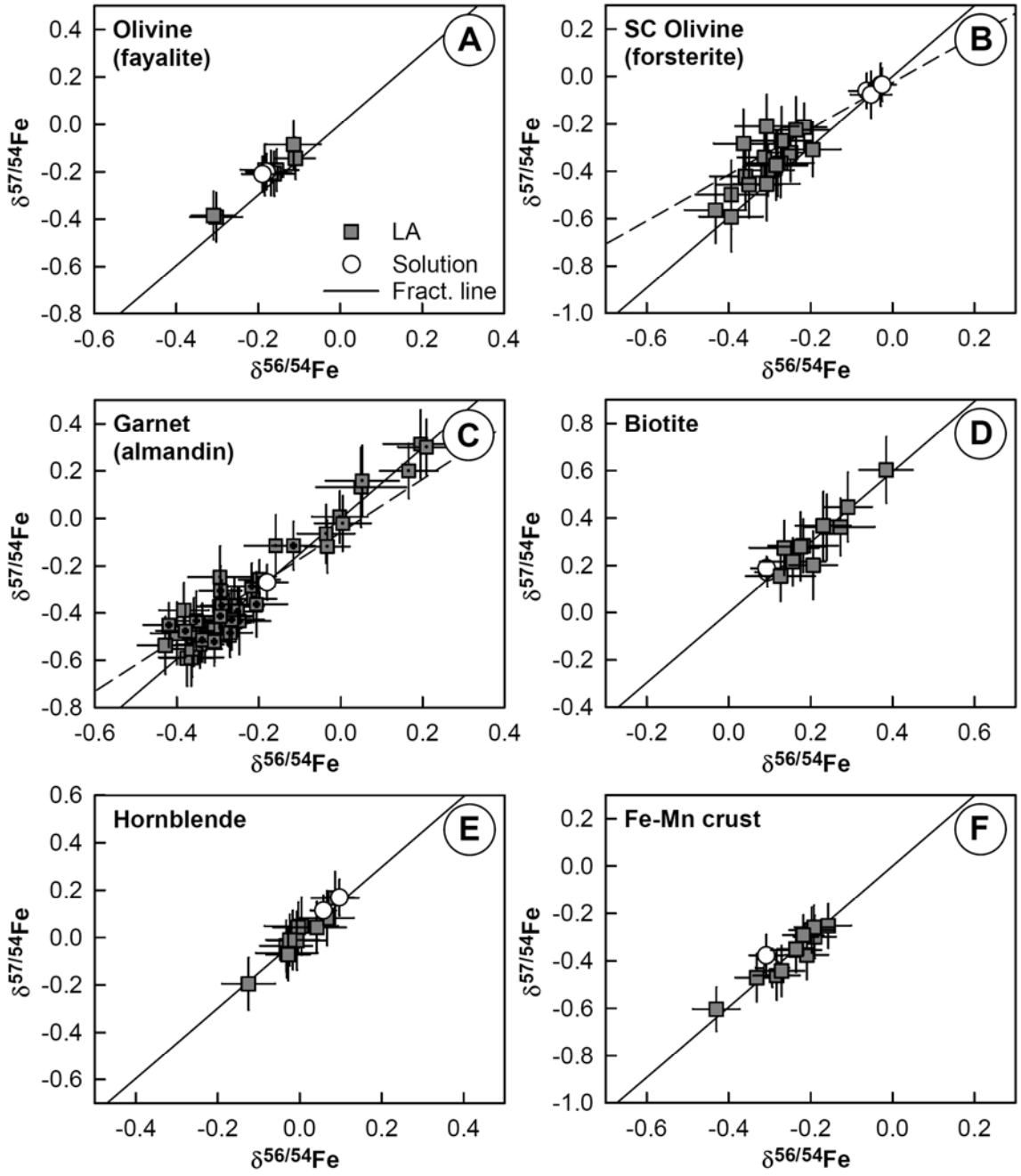

Figure 1: Three-isotope plots for the analysed sample materials showing normalized isotope ratios obtained by UV fs LA-ICP-MS using the raster-mode (closed squares) and conventional solution nebulization ICP-MS (open circles). With the exception of forsterite (SC Olivine) and garnet, all data plot along the mass-dependent fractionation line demonstrating the absence of molecular or elemental interferences during fs LA-ICP-MS. The LA data of forsterite (SC Olivine) **(B)** are shifted towards lower values along a vector with the slope of ~1 (dashed line) indicating a significant under-correction of the isobaric interference of ^{54}Cr on ^{54}Fe if compared to solution ICP-MS data. The garnet crystal was analysed preferentially at the rim (crossed squares) and the interior (dotted squares) **(C)**.

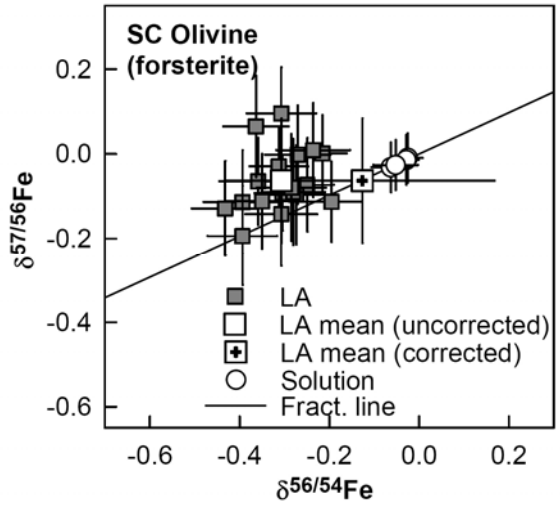

Figure 2: Plot of $\delta^{56/54}$Fe versus $\delta^{57/56}$Fe for the SC Olivine with a high Cr concentration (^{54}Cr/^{54}Fe = 0.0011). Insufficient ^{54}Cr correction on ^{54}Fe results in $\delta^{56/54}$Fe data which differ from the true value, i.e. the solution value, whereas the $\delta^{57/56}$Fe values are unaffected. LA reveals $\delta^{56/54}$Fe values which are 0.3‰ lower on average compared to the solution $\delta^{56/54}$Fe values. Because Fe isotopes fractionate mass-dependent, $\delta^{56/54}$Fe can be calculated from the unaffected $\delta^{57/56}$Fe value by multiplying with a factor of 1.9944, which corresponds to the mass difference between ^{56}Fe and ^{54}Fe relative to the mass difference between ^{57}Fe and ^{56}Fe and an exponential fractionation law. This approach reveals an inferred mean $\delta^{56/54}$Fe value that is close to $\delta^{56/54}$Fe obtained by solution ICP-MS.

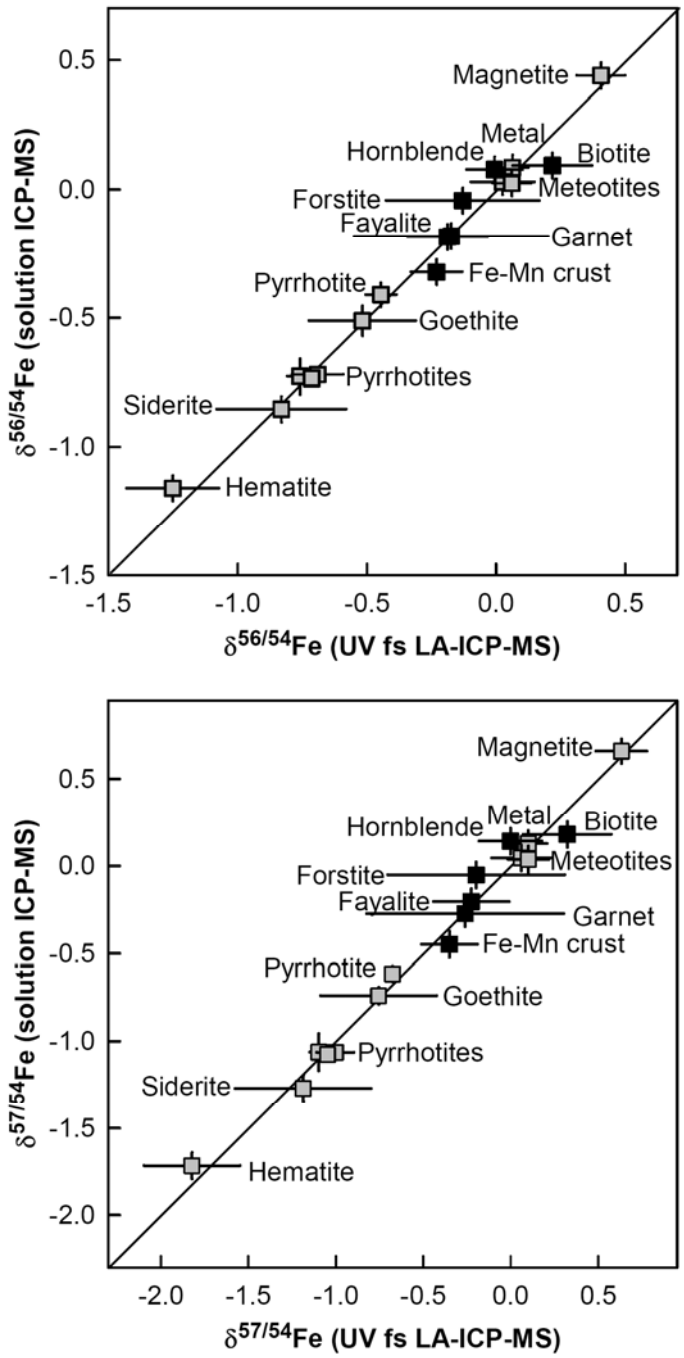

Figure 3: Comparison of mean $\delta^{56/54}$Fe and $\delta^{57/54}$Fe values obtained by *in situ* UV fs LA-ICP-MS with those measured by solution ICP-MS. Gray data points were published in Horn et al. (2006), black data points are from this study. All LA data agree with the data obtained from solution within their respective errors. While maintaining high precision and accuracy, the reliability of matrix-independent calibration is now validated for metals, oxides, hydroxides, carbonates, sulfides, silicates and the complex matrix of Mn-Fe crusts. Large error bars for some of the LA data are caused by heterogeneous sample material. Due to high Cr concentrations in forsterite and garnet, the $\delta^{56/54}$Fe and $\delta^{57/54}$Fe values are inferred from $\delta^{57/56}$Fe values which increase their errors.

Table 1

Instrumental parameters of the Neptune MC-ICP-MS for UV fs LA

Cool gas: Ar [L min^{-1}]	15.00
Auxiliary gas: Ar [L min^{-1}]	0.7-1.0
Sample gas: Ar [L min^{-1}]	0.7-0.8
Add gas: He [L min^{-1}]	0.9-1.0
RF generator power [W]	1200
Acceleration voltage [V]	-10000
Extraction [V]	-1200
Focus [V]	-600
Sample cone	Ni, orifice 1.1 mm diameter
Skimmer cone	H-type, Ni, orifice 0.8 mm diameter
Mass resolution	~8000
Amplifiers [Ω]	10^{11}
Faraday cup setup:	
^{52}Cr (L4),^{54}Fe (L2),^{56}Fe (Central),^{57}Fe (H1),^{58}Fe (H2),^{60}Ni (H4)	
Cycle integration time [s]	2
Number of cycles	40-80

Table 2

Chemical composition in weight percent with anhydrous, F and Cl excluded

Sample	Olivine[a] (fayalite)	SC Olivine[b] (forsterite)	Garnet	Biotite	Hornblende[c]	Fe-Mn Crust[d]
SiO_2	30.72	40.54	37.63	35.04	43.80	6.40
Al_2O_3	-	0.03	21.21	18.10	9.22	-
TiO_2	-	0.01	0.01	2.88	1.53	-
Cr_2O_3	-	0.02	0.11	-	0.01	-
MgO	3.64	48.82	4.96	7.14	11.23	1.11
FeO	64.75	9.81	33.63	21.88	17.16	12.65
MnO	1.10	0.14	0.60	0.33	0.39	20.10
CaO	0.04	0.08	2.40	-	11.91	1.25
Na_2O	-	0.02	0.02	0.08	1.17	-
K_2O	-	-	-	9.40	1.16	-
Total	100.25	99.39	100.58	95.09	97.55	41.51

The average chemical compositions of fayalite, forsterite, hornblende and the Fe-Mn crust are published ([a]Frost et al., 2007; [b]Galer and O'Nions, 1989; [c]Villa and von Blanckenburg, 1991; [d]von Stackelberg et al., 1984). The compositions of biotite B-4B and garnet were obtained by electron microprobe. Cl, F and anhydrous have not been analysed and are unconsidered in the total sums.

Table 3

Repetition rates and signal intensities for UV fs LA-ICP-MS

Sample	IRMM-014/ Puratronic	SC Olivine (forsterite)	Olivine (fayalite)	Biotite	Hornblende	Garnet	Fe-Mn Crust
Repetition rate [Hz]	2-5	90-350	60	50-70	60	100	20
Ion beam on $^{56}Fe^{a}$ [V]	5-10	5	10	5	9	12	8

[a]Faraday cups are equipped with $10^{11}\Omega$ resistors.

Table 4

Mean Fe isotope data obtained by UV fs LA-ICP-MC and solution ICP-MS

	UV fs LA-ICP-MS						Solution ICP-MS		
Sample material	$\delta^{56/54}Fe_{mean}$	$\delta^{57/54}Fe_{mean}$	$\delta^{57/56}Fe_{mean}$	$\delta^{56/54}Fe^{*}_{mean}$	$^{54}Cr/^{54}Fe_{mean}$	n	$\delta^{56/54}Fe_{mean}$	$\delta^{57/54}Fe_{mean}$	n
Puratronic (pure iron)	0.08 ± 0.09	0.12 ± 0.14	0.04 ± 0.08	0.08 ± 0.17	0.0000035	83	0.09	0.13	4
Olivine (fayalite)	-0.19 ± 0.15	-0.23 ± 0.22	-0.04 ± 0.07	-0.08 ± 0.15	0.0000019	8	-0.18	-0.21	2
SC Olivine (forsterite)	-0.31 ± 0.13	-0.37 ± 0.23	-0.06 ± 0.15	-0.13 ± 0.30	0.0011	18	-0.04	-0.05	4
Garnet total	-0.23 ± 0.34	-0.32 ± 0.49	-0.09 ± 0.19	-0.17 ± 0.38	0.0010	44	-0.18	-0.27	1
rim	-0.28 ± 0.13	-0.40 ± 0.20	-0.12 ± 0.13	-0.25 ± 0.25	0.0010	23			
interior	0.01 ± 0.30	0.05 ± 0.37	0.04 ± 0.13	0.07 ± 0.25	0.0010	11			
Biotite	0.22 ± 0.15	0.32 ± 0.25	0.12 ± 0.13	0.24 ± 0.26	0.000017	11	0.09	0.18	2
Hornblende	-0.01 ± 0.11	0.00 ± 0.18	0.00 ± 0.08	0.01 ± 0.16	0.000082	12	0.08	0.14	2
Fe-Mn Crust	-0.23 ± 0.10	-0.35 ± 0.16	-0.12 ± 0.08	-0.24 ± 0.16	0.0000077	11	-0.30	-0.40	2

UV fs LA-ICP-MS and solution ICP-MS data are given as mean values in permil [‰], though all data are plotted in Figure 1. Uncertainties give the external repeatability as 2 standard deviations yielded by multiple analyses (n). $\delta^{56/54}Fe^{*}$mean values are calculated from $\delta^{57/56}Fe$ values by multiplying with a factor of 1.9944, which corresponds to the mass difference between ^{56}Fe and ^{54}Fe relative to the mass difference between ^{57}Fe and ^{56}Fe. $\delta^{56/54}Fe^{*}$ and $\delta^{57/56}Fe$ values are preferred if $^{54}Cr/^{54}Fe$ > 0.0001 as the Cr correction becomes unsatisfactory (Schoenberg and von Blanckenburg, 2005). Average solution ICP-MS data for fayalite were published by Frost et al. (2007).